Engineered ACE2 counteracts vaccine-evading SARS-CoV-2 Omicron variant

Nariko Ikemura[1]*, Shunta Taminishi[1]*, Tohru Inaba[2]*, Takao Arimori[3]*, Daisuke Motooka[4]*, Kazutaka Katoh[5]*, Yuhei Kirita[6], Yusuke Higuchi[1], Songling Li[5], Yumi Itoh[7], Yuki Ozaki[4], Shota Nakamura[4], Satoaki Matoba[1], Daron M Standley[5] † , Toru Okamoto[7] † , Junichi Takagi[3] † , Atsushi Hoshino[1] †

[1] Department of Cardiovascular Medicine, Graduate School of Medical Science, Kyoto Prefectural University of Medicine, Kyoto, Japan.
[2] Department of Infection Control and Molecular laboratory Medicine, Graduate School of Medical Science, Kyoto Prefectural University of Medicine, Kyoto, Japan.
[3] Laboratory of Protein Synthesis and Expression, Institute for Protein Research, Osaka University, Osaka, Japan.
[4] Department of Infection Metagenomics, Research Institute for Microbial Diseases, Osaka University, Osaka, Japan.
[5] Department of Genome Informatics, Research Institute for Microbial Diseases, Osaka University, Osaka, Japan.
[6] Department of Nephrology, Graduate School of Medical Science, Kyoto Prefectural University of Medicine, Kyoto, Japan.
[7] Institute for Advanced Co-Creation Studies, Research Institute for Microbial Diseases, Osaka University, Osaka, Japan.

* These authors contributed equally to this work.
† Corresponding author. Email: a-hoshi@koto.kpu-m.ac.jp (A.H.); takagi@protein.osaka-u.ac.jp (J.T.); toru@biken.osaka-u.ac.jp (T.O.); standley@biken.osaka-u.ac.jp (D.M.S.)

One Sentence Summary

Omicron carrying ~30 mutations in the spike exhibits the serious immune evasion partly due to NTD mutations, but it remains highly susceptible to the blockade by the engineered ACE2.

Abstract

The novel SARS-CoV-2 variant, Omicron (B.1.1.529) contains an unusually high number of mutations (>30) in the spike protein, raising concerns of escape from vaccines, convalescent sera and therapeutic drugs. Here we analyze the alteration of neutralizing titer with Omicron pseudovirus. Sera of 3 months after double BNT162b2 vaccination exhibit approximately 18-fold lower neutralization titers against Omicron. Convalescent sera from Alpha and Delta patients allow similar levels of breakthrough by Omicron. However, some Delta patients have relatively preserved neutralization efficacy, comparable to 3-month double BNT162b2 vaccination. Domain-wise analysis using chimeric spike revealed that this efficient

evasion was, at least in part, caused by multiple mutations in the N-terminal domain. Omicron escapes the therapeutic cocktail of imdevimab and casirivimab, whereas sotrovimab, which targets a conserved region to avoid viral mutation, remains effective against Omicron. The ACE2 decoy is another virus-neutralizing drug modality that is free, at least in theory, from mutational escape. Deep mutational analysis demonstrated that, indeed, the engineered ACE2 overcomes every single-residue mutation in the receptor-binding domain, similar to immunized sera. Like previous SARS-CoV-2 variants, Omicron and some other sarbecoviruses showed high sensitivity against engineered ACE2, confirming the therapeutic value against diverse variants, including those that are yet to emerge.

INTRODUCTION

The novel variant B.1.1.529 was detected in Botswana on November 11th and spread rabidly and globally. On November 26th, the World Health Organization (WHO) classified B.1.1.529 as the Omicron variant of concern (VOC). Omicron possesses 26 to 32 mutations, 3 deletions and one insertion in the spike protein. Among these, 15 mutations are located in the receptor binding domain (RBD) (1). Spike mutations have the potential to enhance transmissibility, enable immune evasion, or both (2). Compared to previous variants, Omicron contains far more mutations in the spike and these mutations could dramatically alter the characteristics of SARS-CoV-2. According to routine surveillance data from South Africa, Omicron has higher transmission and risk of reinfection due to immune evasion (1). In addition, multiple mutations in the RBD can impact escape from therapeutic monoclonal antibodies, even in cocktail regimen (3, 4).

We previously developed an engineered ACE2 containing mutations to enhance the affinity toward SARS-CoV-2 spike that showed virus-neutralizing capacity comparable to therapeutic monoclonal antibodies (3). The advantage of the ACE2-based decoy is its resistance to virus escape mutations. Mutant spikes escaping from ACE2 decoy may appear, but they would have limited binding affinity toward the native ACE2 receptors on host cells, making such resultant viruses unfit to propagate due to greatly reduced or even no infectivity. In fact, the engineered ACE2 successfully neutralized previous variant viruses and even SARS-CoV-1, and showed no signs of vulnerability to escape mutants when added at suboptimal concentration during the long-term culture (5).

In this report, we examined the antigenic alteration of Omicron and demonstrate that Omicron does evade neutralization by vaccinated and convalescent sera. Mutations in the RBD dominantly contributed to the ability of Omicron to escape, although those in the N-terminal domain (NTD) also contributed to some extent. A broad range of antibodies failed to neutralize Omicron, including a cocktail of imdevimab and casirivimab. However, the ACE2 decoy remained effective to Omicron as well as other sarbecoviruses.

RESULTS

Genetic and epidemic characteristics of Omicron

Mutations in the Omicron spike protein are shown in Figure 1A. More than 30 amino acids were identified and compared to other variants of concern (VOC) reported in the GISAID database. We noticed that most

mutations found in the Omicron strain are also present in previous VOCs as a minor population (Fig. 1A). About 70% of mutations are located in the S1 subunit harboring the NTD and RBD, suggesting that mutations in Omicron would influence binding affinity toward neutralizing antibodies, host receptors such ACE2, or both. Phylogenetic analysis of the full-length spike protein demonstrated that the spike protein of the Omicron strain was relatively close to gamma and beta strains compared to other VOC and VOI (Fig. 1B). The time course of dissemination of Omicron in the world has shown that the Delta strain was rapidly exchanged with the Omicron strain in South Africa (Fig. 1C). These data support the notion that mutations in the Omicron spike protein enhance the infection rates.

Omicron evades vaccine and convalescent sera through mutations in the RBD and NTD

To evaluate the infectivity of Omicron, we generated a pseudotyped virus harboring the spike of Omicron and assessed neutralizing activity of BNT162b2 vaccinated and convalescent sera against it. Virus neutralization assay with vaccinated sera obtained from 12 persons 3 months after vaccination with double Pfizer-BioNTech vaccine BNT162b2 showed approximately 18-fold lower neutralization titers against Omicron than the D614G mutation (parental virus) (Fig. 2A and Fig. S1). We also collected convalescent sera before or after the pandemic of the Delta variant. Convalescent sera before the Delta pandemic (December 2020 through January 2021) showed approximately 30-fold reduction and those collected during/after the Delta pandemic (August 2021 through October 2021) exhibited approximately 12-fold reduction. Importantly, among 18 patients during the Delta pandemic, sera from 11 patients exhibited the protective capacity against Omicron being comparable to those of 3 months after double BNT162b2 vaccination against parental virus (NT_{50} value >100) (Fig. 2B, C and Fig. S1).

To examine the contribution of NTD mutations, we made a pseudovirus harboring a chimeric spike that contained Omicron's NTD in parental virus or parental NTD in the Omicron variant. Replacing parental virus NTD with Omicron mildly attenuated the neutralizing effect of vaccinated sera. In contrast, the removal of NTD mutations from Omicron generally increased the susceptibility to the vaccine neutralization (Fig. 2D).

Engineered ACE2 broadly neutralizes SARS-CoV-2 variants, including Omicron and other Sarbecoviruses

We next evaluated the efficacy of neutralizing drugs developed for the Wuhan strain. Currently the cocktail of imdevimab, casirivimab and sotrovimab were approved in Japan. The cocktail showed greatly reduced neutralization activity toward Omicron (> 1,000-fold reduction from Wuhan), whereas that of sotrovimab was preserved (Fig. 3A). We previously reported that engineered ACE2 could neutralize a broad range of SARS-CoV-2 variants including Alpha, Beta, and Gamma (5). Despite far more extensive mutation in the Omicron RBD compared with these previous VOCs, all three high-affinity engineered ACE2-Fc we developed (3N39v4, 3J113v2, and 3J320v2) exhibited high neutralizing efficacy against Omicron at levels indistinguishable or even higher than the original Wuhan strain (Fig. 3B). The concept of engineered ACE2 was independently introduced by several groups and their combination of mutations

were all unique(6, 7). Among these, we tested two different ACE2 mutants reported by Procko and co-workers(6), and both showed similar or better neutralization against Omicron (Fig. S2).

We then examined the breadth of cross-neutralization against other SARS-CoV-2 variants and sarbecoviruses by our engineered ACE2 (Fig. 4A). In addition to Alpha, Beta, and Gamma variants that were previously reported (5), engineered ACE2 (3N39v4) showed similar or better efficacy to Delta, Epsilon, Lambda and Mu, as compared with the original Wuhan strain (Fig. 4B). This high level of inhibition was also observed in SARS-CoV-2 clade Pangolin coronaviruses GD-1(8) and the SARS-CoV-1 clade bat WIV1(9) (Fig.4C). These results indicate that engineered ACE2 has therapeutic potency against a broad range of SARS-CoV-2 variants and sarbecoviruses.

Structural modeling of the binding mode of engineered ACE2 to Omicron RBD

We previously determined the crystal structure of Wuhan RBD complexed with the primary ACE2 mutant, 3N39, carrying seven mutations (i.e. A25V, K26E, K31N, E35K, N64I, L79F, and N90H) (5). K35 forms a direct hydrogen bond with Q493 of the RBD (Fig. 5A), whereas the wild type residue E35 forms an intramolecular salt bridge with K31, making us to speculate that the simultaneous mutations of K31N and E35K played a key role in the affinity enhancement of this mutant. However, Q493 was substituted with Arg in Omicron RBD, which could lower the affinity toward our engineered ACE2 due to electrostatic repulsion with K35. To simulate the biding mode, we built a homology model of Omicron RBD using MODELLER(10) with the Wuhan RBD structure (PDB ID: 7dmu) as an initial model (Fig. 5B). In the complex model, the electrostatic clash between K35 of the ACE2 mutant and R493 of Omicron RBD could easily be avoided by side chain rotation. Furthermore, we found that the side chain of R493 could form a direct hydrogen bond with N31 of ACE2(3N39) instead of K35 (Fig. 5B, inset). Therefore, consistent with the results of the neutralization assay, our engineered ACE2 is expected to have no or little loss of affinity for Omicron RBD.

No evidence of escape mutation in deep mutational scanning of the RBD

To comprehensively analyze the alteration of viral infectivity and escape from neutralizing agents, we performed a deep mutational scan (DMS) of the RBD in the context of full-length spike expressed on human Expi293 cells, followed by incubation with ACE2-harboring a GFP-reporter virion. Although DMS analysis on the spike had been done by Starr et al (11), they used yeast surface display of isolated RBDs which would assess RBD's structural stability and its affinity against ACE2 or neutralizing agents separately. In contrast, our assay monitors the fusion of cell and viral membranes mediated by binding between spike and ACE2 and better mimics the true infection process, albeit in an inverted orientation. The spike library encompassed all 20 amino acid substitutions in the RBD (a.a. P329 to G538) and was transfected in Expi293 cells in a manner where cells typically acquire no more than a single variant (12). After infection of library cells with ACE2-harboring virion, infected GFP-positive cells and control GFP negative cells were harvested with fluorescence-activated cell sorting (FACS) and the library was sequenced with extracted RNA (Fig.6A). DMS experiments were performed in duplicate and correlated well (R^2 = ~0.5; Fig. S3). The

scan without neutralizing agents provides information about infectivity due to all single amino acid mutations in the RBD (Fig. S4A). According to this scanning data, 8 of 15 mutations in the RBD of Omicron may enhance infectivity, whereas 3 mutations (S371L, S373P, S375F) that exist in the conserved region may reduce infection (Fig.6B). Incubation of library cells and ACE2 virion with neutralizing drug and sera succeeded in revealing the mutational patterns that enable evasion. For example, the scan in the presence of casirivimab detected all epitope residues previously reported (13, 14), which confirmed the sensitivity of the assay to detect escape mutations (Fig.6C and Fig. S4B). Some VOCs exhibited partial resistance to neutralization by immunized sera (2), however actual escape is achieved by a combination of mutations, not only by single mutations (15). Consistently, the scan measuring resistance to vaccinated sera revealed that alteration of escape value simply paralleled that of infectivity without irregular enhancements, unlike the case of casirivimab (Fig.6D and Fig. S4C). This result was reproduced by the sera from a different vaccinated individual (Fig. S5). A similar result was also observed in a scan for escape from engineered ACE2 (Fig. 6E and Fig. S4D), which provides evidence that engineered ACE2 neutralizes each single-residue mutation more effectively than monoclonal antibodies.

DISCUSSION

Omicron contains approximately 30 mutations in the spike protein and escapes vaccine, convalescent sera, and some therapeutic antibodies. Although partial cross-neutralization against Omicron was observed in some patients during the Delta pandemic, presumably due to the accumulation of minor mutations, a vaccine specific to Omicron is required to effectively prevent an Omicron pandemic. Our neutralization assay using pseudovirus harboring chimeric spike of Omicron and the original Wuhan strain demonstrated that multiple mutations in the NTD could contribute to reduce neutralization. Previous studies showed that the deletion mutation in the NTD induced escape from isolated NTD-binding neutralizing antibodies (16). According to another report, vaccinated and convalescent sera exhibited weak neutralization titers, even after depletion of RBD-binding antibodies (17). These reports indicate the possibility of NTD-mediated active neutralization by immunized sera, and this study demonstrated that extensive escape of Omicron is achieved by attenuated neutralization by NTD-binding antibodies.

For therapeutic strategies to overcome virus mutation, some antibodies are used in the form of a cocktail and others are designed to target a conserved region, in order to prevent mutational escape. However, Omicron exhibits the ability to pass through combinations of antibodies(3, 4) and acquired mutations even in highly conserved vulnerable sites (S371L, S373P, S375F). These observations provide a sobering outlook for the development of monoclonal antibodies against viruses in the context of escape mutation. In contrast, engineered ACE2 successfully neutralized Omicron and even other sarbecovirus that could form the basis of future SARS-CoV-3 variants. The emergence of Omicron reinforces the difficulty of drug development against viral infection and highlights the strength of ACE2 decoys to counteract COVID-19 mutational escape

MATERIALS AND METHODS

Ethics statement

Blood samples were obtained from hospitalized adults with PCR-confirmed SARS-CoV-2 infection and vaccinated individuals who were enrolled in a prospective cohort study approved by the Clinical Research Review Committee in Kyoto Prefectural University of medicine (ERB-C-1810-2, ERB-C-1949-1). All human subjects provided written informed consent.

Omicron genetic and epidemic analysis

Amino acid mutation frequencies in the spike protein for each variant (Alpha = 1,138,704, Beta = 40,135, Gamma = 117,200, Delta = 3,441,137, and Omicron = 5,469 sequences) were extracted from the report of outbreak.info (https://outbreak.info/compare-lineages?pango=Delta&pango=Omicron&pango=Alpha&pango=Beta&pango=Gamma&gene=S&threshold=0.2&nthresh=1&sub=false&dark=true%29.%20Accessed%2017%20December%202021.) as of December 17, 2021. Mutation frequencies of each amino acid substitution which was observed in Omicron were plotted using "corrplot" package in R. Time course of variant distribution was analyzed by Nextclade ver 1.7.0 (https://joss.theoj.org/papers/10.21105/joss.03773) from SARS-CoV-2 nucleic acid sequences which were downloaded from GISAID database as of December 17, 2021. A phylogenetic tree of spike protein from SARS-CoV-2 variants and relatives were inferred based on full-length amino acid sequences taken from GISAID, genbank, National Genomics Data Center and the database of SARS-CoV-2 variants by Stanford HIVDB team. The neighbor joining method(18) was applied to a distance matrix estimated by the maximum likelihood method. To perform multiple sequence alignment of spike proteins 6,000,693 spike protein amino acid sequences were downloaded from GISAID on Dec 14, 2021. The frequency of all unique RBD regions (defined as R319-541F) were determined for each major variant (as defined in https://en.wikipedia.org/wiki/Variants_of_SARS-CoV-2), and the most frequent instance within a variant was used as a representative. The sequences were multiply aligned by MAFFT(19) with the corresponding RBD regions from PG-GD1, VIW1 and CoV-1. The MSA was rendered using an in-house script to show only positions non-identical to the Wuhan strain.

Cell culture

Lenti-X 293T cells (Clontech) and its derivative, 293T/ACE2 cells were cultured at 37 °C with 5% CO_2 in Dulbecco's modified Eagle's medium (DMEM, WAKO) containing 10% fetal bovine serum (Gibco) and penicillin/streptomycin (100 U/ml, Invitrogen). All the cell lines were routinely tested negative for mycoplasma contamination.

Protein synthesis and purification

Monoclonal antibodies and engineered ACE2 were expressed using the Expi293F cell expression system (Thermo Fisher Scientific) according to the manufacturer's protocol. Fc-fused proteins were purified from conditioned media using the rProtein A Sepharose Fast Flow (Cytiva), respectively. Fractions containing target proteins were pooled and dialyzed against phosphate buffered saline (PBS).

Pseudotyped virus neutralization assay

Pseudotyped reporter virus assays were conducted as previously described (5). A plasmid coding SARS-CoV-2 Spike was obtained from addgene #145032 and Omicron's mutations and ΔC19 deletion (with 19 amino acids deleted from the C terminus) was cloned into pcDNA4TO (Invitrogen) (20). Spike-pseudovirus with a luciferase reporter gene was prepared by transfecting plasmids (OmicronΔC19, psPAX2-IN/HiBiT (21), and pLenti firefly) into LentiX-293T cells with Lipofectamine 3000 (Invitrogen). After 48 hr, supernatants were harvested, filtered with a 0.45 μm low protein-binding filter (SFCA), and frozen at –80 °C. The 293T/ACE2 cells were seeded at 10,000 cells per well in 96-well plate. HiBit value-matched Pseudovirus and three-fold dilution series of serum or therapeutic agents were incubated for 1 hr, then this mixture was administered to ACE2/293T cells. After 1 hr pre-incubation, medium was changed and cellular expression of luciferase reporter indicating viral infection was determined using ONE-Glo™ Luciferase Assay System (Promega) in 48 hr after infection. Luminescence was read on Infinite F200 pro system (Tecan). The assay of each serum was performed in triplicate, and the 50% neutralization titer was calculated using Prism 9 (GraphPad Software).

Library construction, FACS, and Illumina sequencing analysis

Saturation mutagenesis was focused on the original Wuhan strain spike residues F329 to C538 forming the RBD. Pooled oligo with degenerate NNK codon was synthesized by Integrated DNA Technologies, Inc. Synthesized oligo was extended by overlap PCR and cloned into pcDNA4TO HMM38-HA-full length S plasmid. Transient transfection conditions were used that typically provide no more than a single coding variant per cell(12). Expi293F cells at 2×10^6/ml were transfected with a mixture of 3 ng of library plasmid with 1.5 μg of pMSCV as a junk plasmid using ExpiFectamine (Thermo Fisher Scientific). Twenty-four hours after transfection, cells were incubated with ACE2-harboring GFP reporter virion. In case of escape analysis, cells were pre-incubated with neutralizing agents for 1 hr. One-hour incubation with ACE2 virion, the medium was replaced and cells were collected 24 hours after infection for FACS. Cells were washed twice with PBS-BSA and then co-stained for 20 min with anti-HA Alexa Fluor 647 (clone TANA2,1/4000 dilution; MBL). Cells were again washed twice before sorting on a MA900 (Sony). Dead cells, doublets, and debris were excluded by first gating on the main population by forward/side scattering. From the HA positive (Alexa Fluor 647) population, GFP-positive and -negative cells were collected. The total numbers of collected cells were ~2 million cells for each group. Total RNA was extracted from collected cells TRIzol (Life Technologies) and Direct-zol RNA MiniPrep (Zymo Research Corporation) according to the manufacturer's protocol. First-strand complementary DNA (cDNA) was synthesized with Accuscript (Agilent) primed with a gene-specific oligonucleotide. Library was designed for 3 sections separately in the RBD and pooled. After cDNA synthesis, each library was amplified with specific primers. Following a second round of PCR, primers added adapters for annealing to the Illumina flow cell and sequencing primers, together with barcodes for experiment identification. The PCR products were sequenced on an Illumina NovaSeq 6000 using a 2 × 150 nucleotide paired-end protocol in Department of Infection

Metagenomics, Research Institute for Microbial Diseases, Osaka University. Data were analyzed comparing the read counts with each group normalized by wild type sequence read-count. Log10 enrichment ratios for all the individual mutations were calculated and normalize by subtracting the log10 enrichment ratio for the WT sequence across the same PCR-amplified fragment.

Statistical analysis

Neutralization measurements were done in technical triplicates and relative luciferase units were converted to percent neutralization and plotted with a non-linear regression model to determine IC50/ID50 values using GraphPad PRISM software (version 9.0.0). Comparisons between two groups of paired data were made with paired *t* test.

SUPPLEMENTARY MATERIALS

Figs. S1 to S5

References AND NOTES

1. Pulliam JRC *et al.*, Increased risk of SARS-CoV-2 reinfection associated with emergence of the Omicron variant in South Africa. *medRxiv* 2021:2021.11.11.21266068. DOI:10.1101/2021.11.11.21266068.
2. K. Uriu *et al.*, Neutralization of the SARS-CoV-2 Mu Variant by Convalescent and Vaccine Serum. *N Engl J Med* 10.1056/NEJMc2114706 (2021).
3. E. Cameroni *et al.*, Broadly neutralizing antibodies overcome SARS-CoV-2 Omicron antigenic shift. *bioRxiv* 10.1101/2021.12.12.472269 (2021).
4. A. Wilhelm *et al.*, Reduced Neutralization of SARS-CoV-2 Omicron Variant by Vaccine Sera and Monoclonal Antibodies. *medRxiv* 10.1101/2021.12.07.21267432 (2021).
5. Y. Higuchi *et al.*, Engineered ACE2 receptor therapy overcomes mutational escape of SARS-CoV-2. *Nat Commun* **12**, 3802 (2021).
6. K. K. Chan *et al.*, Engineering human ACE2 to optimize binding to the spike protein of SARS coronavirus 2. *Science* **369**, 1261-1265 (2020).
7. A. Glasgow *et al.*, Engineered ACE2 receptor traps potently neutralize SARS-CoV-2. *Proc Natl Acad Sci U S A* **117**, 28046-28055 (2020).
8. T. T. Lam *et al.*, Identifying SARS-CoV-2-related coronaviruses in Malayan pangolins. *Nature* **583**, 282-285 (2020).
9. X. Y. Ge *et al.*, Isolation and characterization of a bat SARS-like coronavirus that uses the ACE2 receptor. *Nature* **503**, 535-538 (2013).
10. A. Sali, T. L. Blundell, Comparative protein modelling by satisfaction of spatial restraints. *J Mol Biol* **234**, 779-815 (1993).
11. T. N. Starr *et al.*, Deep Mutational Scanning of SARS-CoV-2 Receptor Binding Domain Reveals

Constraints on Folding and ACE2 Binding. *Cell* **182**, 1295-1310 e1220 (2020).
12. K. K. Chan, T. J. C. Tan, K. K. Narayanan, E. Procko, An engineered decoy receptor for SARS-CoV-2 broadly binds protein S sequence variants. *Sci Adv* **7** (2021).
13. A. Baum *et al.*, Antibody cocktail to SARS-CoV-2 spike protein prevents rapid mutational escape seen with individual antibodies. *Science* **369**, 1014-1018 (2020).
14. T. N. Starr *et al.*, Prospective mapping of viral mutations that escape antibodies used to treat COVID-19. *Science* **371**, 850-854 (2021).
15. Q. Li *et al.*, SARS-CoV-2 501Y.V2 variants lack higher infectivity but do have immune escape. *Cell* **184**, 2362-2371 e2369 (2021).
16. K. R. McCarthy *et al.*, Recurrent deletions in the SARS-CoV-2 spike glycoprotein drive antibody escape. *Science* **371**, 1139-1142 (2021).
17. A. J. Greaney *et al.*, Antibodies elicited by mRNA-1273 vaccination bind more broadly to the receptor binding domain than do those from SARS-CoV-2 infection. *Sci Transl Med* **13** (2021).
18. N. Saitou, M. Nei, The neighbor-joining method: a new method for reconstructing phylogenetic trees. *Mol Biol Evol* **4**, 406-425 (1987).
19. K. Katoh, D. M. Standley, MAFFT multiple sequence alignment software version 7: improvements in performance and usability. *Mol Biol Evol* **30**, 772-780 (2013).
20. T. Giroglou *et al.*, Retroviral vectors pseudotyped with severe acute respiratory syndrome coronavirus S protein. *J Virol* **78**, 9007-9015 (2004).
21. S. Ozono, Y. Zhang, M. Tobiume, S. Kishigami, K. Tokunaga, Super-rapid quantitation of the production of HIV-1 harboring a luminescent peptide tag. *J Biol Chem* **295**, 13023-13030 (2020).

ACKNOWLEDGEMENTS

We would like to thank Takaaki Nakaya (Kyoto Prefectural University of Medicine) for helpful discussion; Kenzo Tokunaga (Department of Pathology, National Institute of Infectious Diseases) for kind gift of plasmid coding psPAX2-IN/HiBiT. Funding: This work was supported by Japan Agency for Medical Research and Development (AMED), Research Program on Emerging and Re-emerging Infectious Diseases under JP 21fk0108465h0001 (A.H., J.T. and T.O.), Platform Project for Supporting Drug Discovery and Life Science Research (Basis for Supporting Innovative Drug Discovery and Life Science Research) under JP21am0101075 (J.T.), JP21am0101108 (D.M.S) and grant from Mochida Memorial Foundation for Medical and Pharmaceutical Research (A.H), ,SENSHIN Medical Research Foundation (N.I). **Author contribution:** A.H. designed the research; N.I. and Y.H. performed pseudovirus neutralization assay; N.I, S.T. and Y.H. performed deep mutational analysis; T.I. provided clinical samples of vaccinated and convalescent sera; Y.K., D.M., Y.O., and S.N. performed and analyzed next-generation sequencing; T.A., J.T. purified and prepared the proteins; T.A. performed structure analysis; K.K., S.L. and D.M.S. conducted phylogenetic analysis and manage SpikeAtlas database; Y.I. and T.O. conducted SARS-CoV-2 experiments in the cell culture; D.M.S., T.O., J.T., and A.H. supervised the research; A.H., J.T., and

T.O. wrote the manuscript; all authors discussed the results and commented on the manuscript. **Competing interests:** Authors declare that they have no competing interests. **Data and materials availability:** All unique/stable reagents generated in this study are available with a completed Materials Transfer Agreement. Deep mutational scan data has been deposited at SpikeDB (https://sysimm.ifrec.osaka-u.ac.jp/sarscov2_dms/).

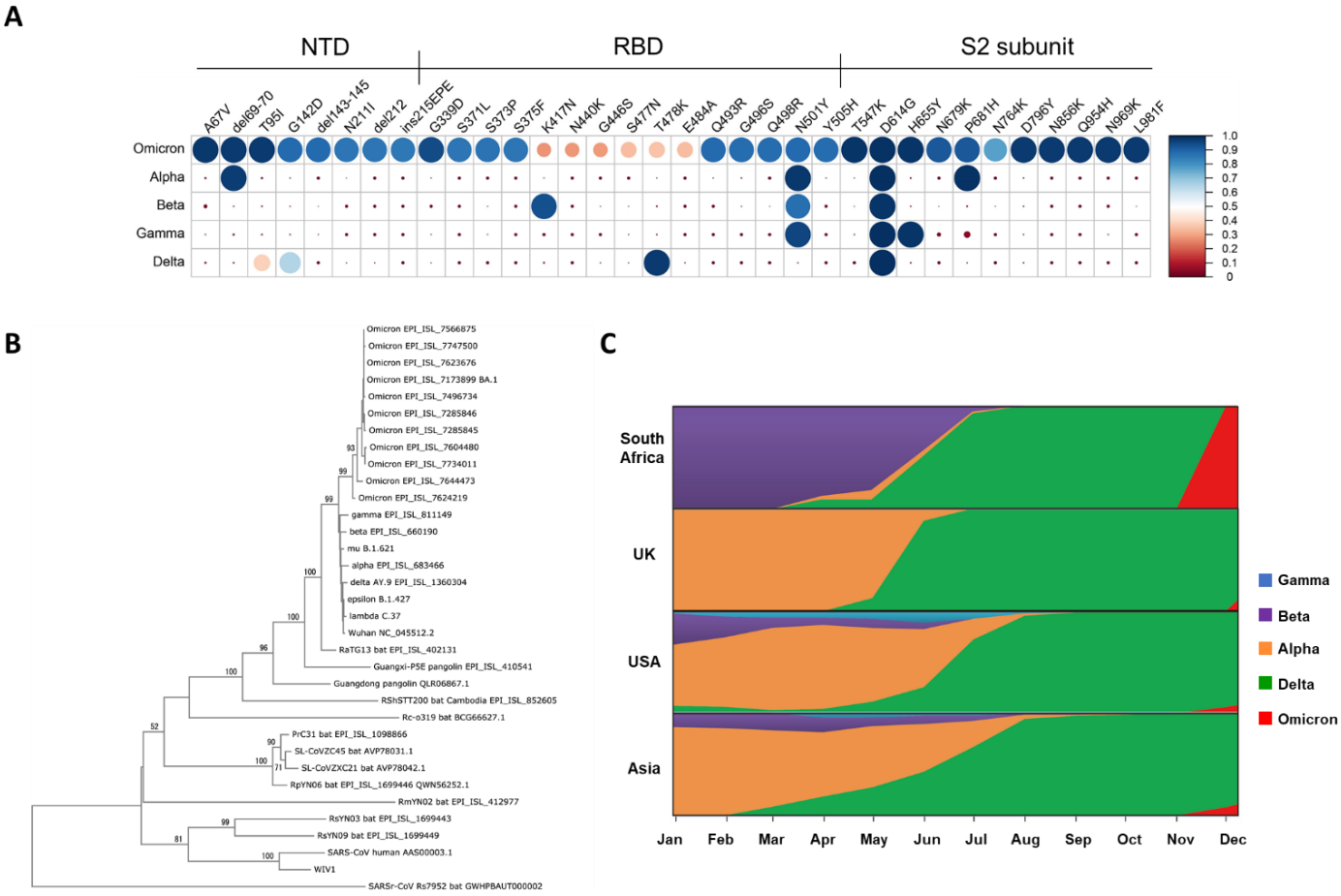

Fig. 1. Emergence of Omicron (B.1.1.529) (**A**) Amino Acid mutations of S protein between SARS-CoV-2 strains. Mutation rate of each amino acid substitution in spike protein which was observed in Omicron were calculated using SARS-CoV-2 sequences reported in GISAID as 17th Dec 2021 (Alpha = 1,138,704, Beta = 40,135, Gamma = 117,200, Delta = 3,441,137, and Omicron = 5,469 sequences). (**B**) Phylogenetic tree of spike protein from variants of SARS-CoV-2 and relatives. Accession number or lineage name is shown for each sequence. Bootstrap values larger than 50% are shown at the corresponding branches. (**C**) Relative proportion of variant cases during 2021 in South Africa, United Kingdom, North America, and Asia.

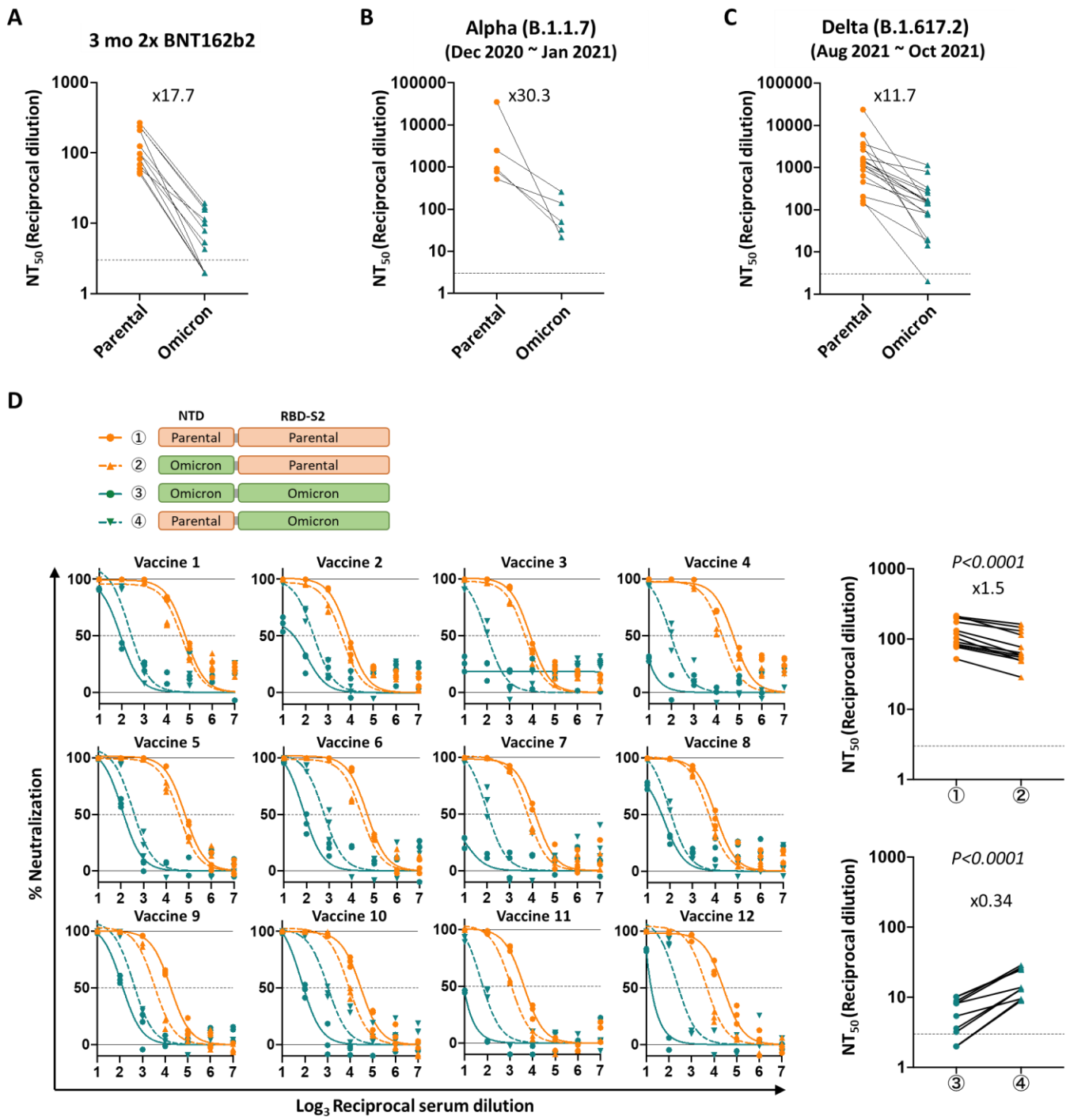

Fig. 2. Neutralization assay with Omicron pseudovirus. (**A-C**) The reciprocal dilution of 50% virus neutralization (NT_{50}) was determined for sera of 3-month double BNT162b2 vaccination (A), convalescent sera from 5 patients infected with Alpha (B) and 18 patients infected with Delta (C) in 293T/ACE2 cells. (**D**) Neutralization efficacy of 12 individual vaccinated sera against parental virus (D614G mutation), parental virus with replacement of Omicron's NTD, Omicron, and Omicron with parental NTD in 293T/ACE2 cells. The NT_{50} was summarized in the right panel. n = 3 technical replicates. Two-tailed *P* values were calculated. Dotted lines indicate detection limit.

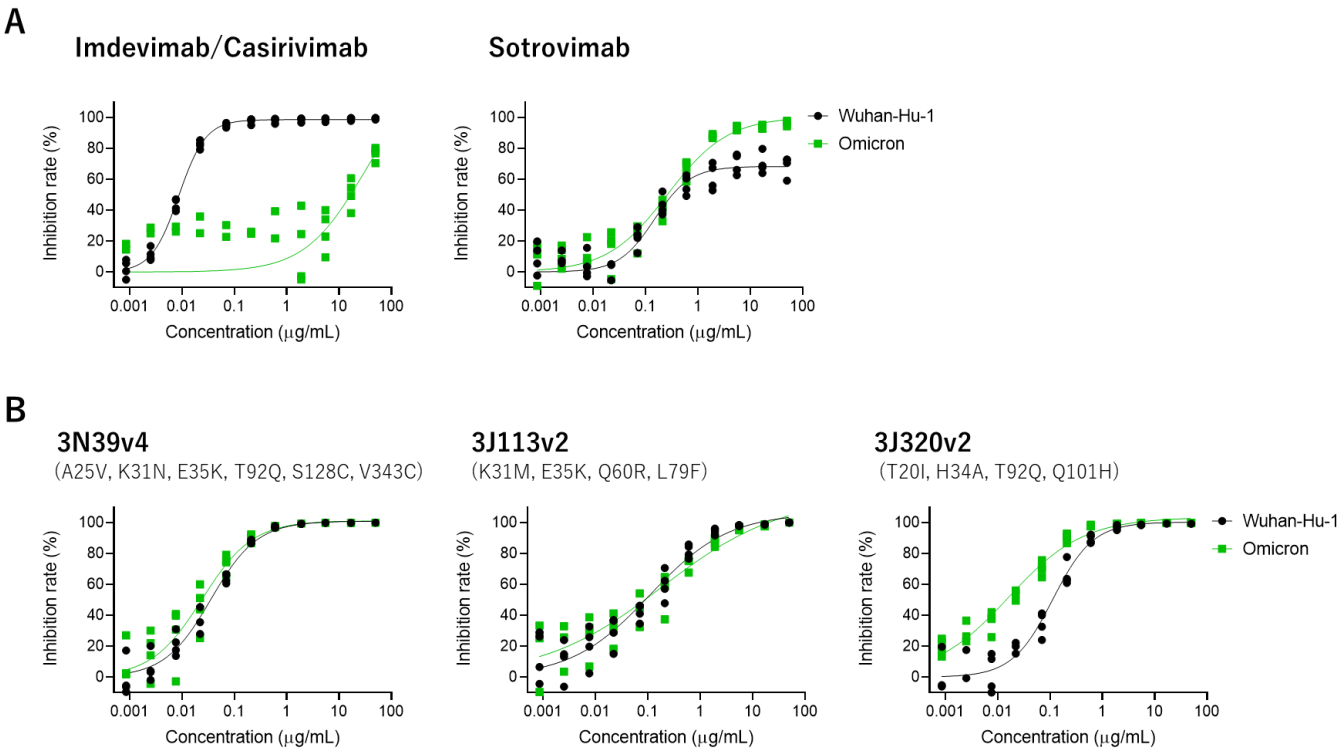

Fig. 3. Neutralization assay for monoclonal antibodies and ACE2 decoy. (**A** and **B**) Neutralization efficacy of the cocktail of imdevimab and casirivimab and sotrovimab against Omicron pseudovirus (A) and the engineered ACE2 (B) in 293T/ACE2 cells. n = 4 technical replicates. The indicated concentrations of imdevimab and casirivimab were applied in a 1:1 ratio.

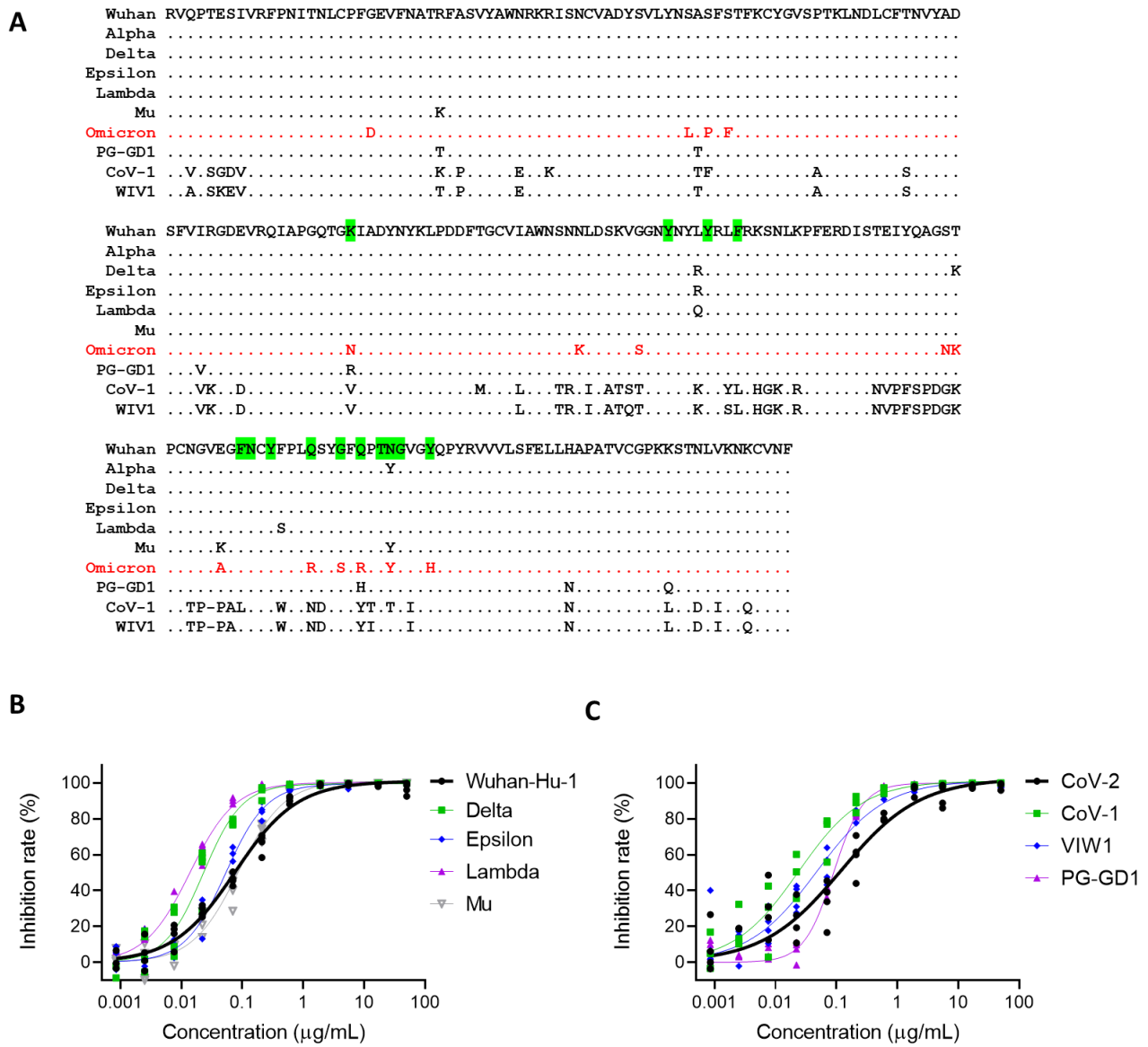

Fig. 4. Neutralization assay for ACE2 decoy with pseudovirus of SARS-CoV-2 variants and sarbecoviruses. (**A**) Alignment of amino acid sequences of sarbecovirus RBDs used in this study. ACE2 contacts are highlighted by green based on the crystal structure 6M0J. (**B** and **C**) Neutralization efficacy of the engineered ACE2(3N39v4) against previous SARS-CoV-2 variants (B), SARS-CoV-1 and other sarbecovirus (C) in 293T/ACE2 cells. n = 4 technical replicates.

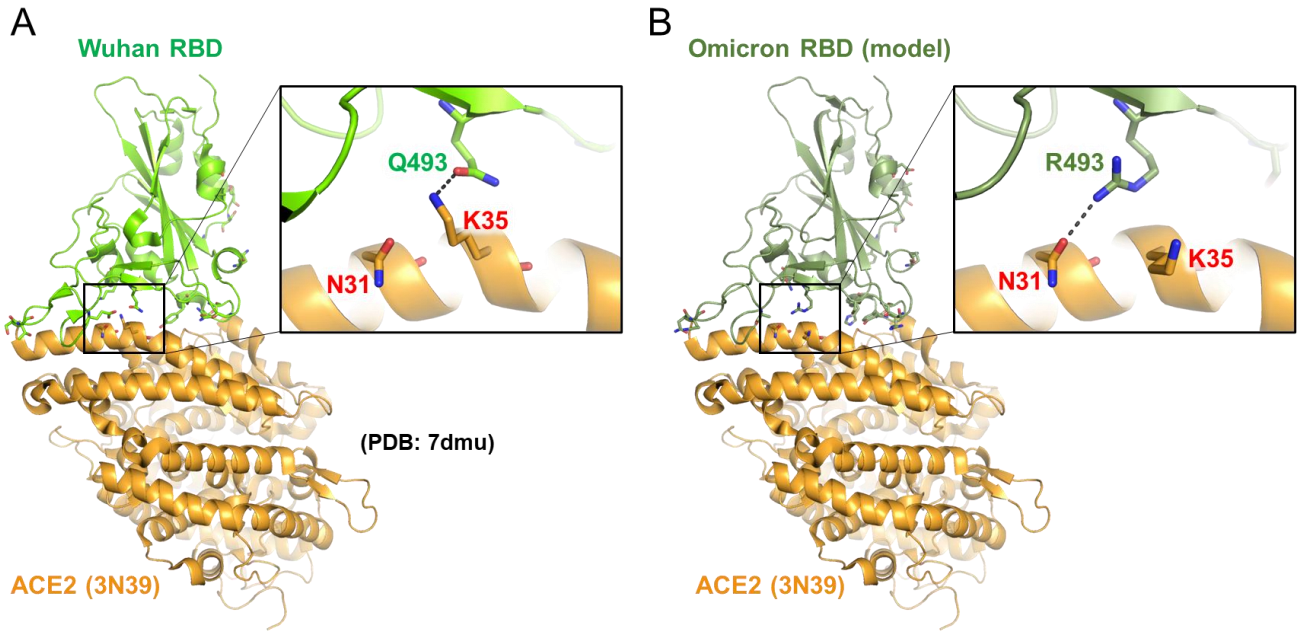

Fig. 5. Difference in the interaction mode of Wuhan RBD and Omicron RBD to ACE2 mutant. (**A** and **B**) Crystal structure of the ACE2 mutant-Wuhan RBD complex (A) and modeled structure of the ACE2 mutant-Omicron RBD complex using MODELLER (B). Residues mutated in Omicron are shown as stick models. Close-up views showing the interaction of the ACE2 mutant with Q493 of Wuhan RBD or R493 of Omicron RBD via the K31N/E35K mutation site are provided in the insets. Observed (A) or hypothetical (B) hydrogen-bonding interactions are indicated by dashed lines.

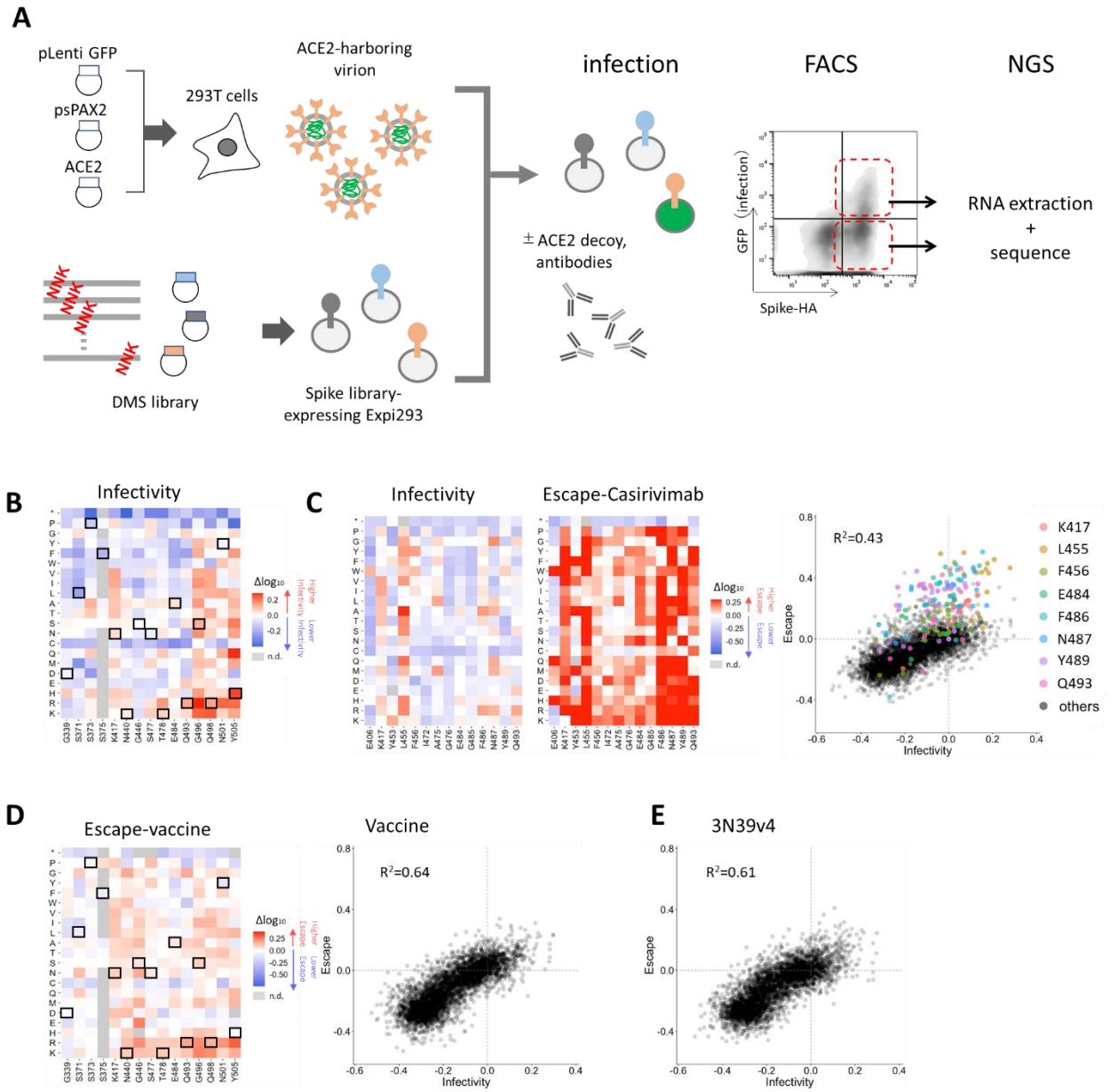

Fig. 6. Deep mutational scan identified no single residue mutation to induce escape from engineered ACE2. (**A**) Schematic of the deep mutational scanning to evaluate infectivity and escape from neutralizing agents. (**B**) Heatmaps illustrating how all single mutations that Omicron obtains affect its infectivity. Open squares are Omicron-carrying mutation. (**C**) Heatmaps showing the alteration of infectivity and escape value from casirivimab in casirivimab antigen sites of the spike protein (left). Correlation in mutation effects on infectivity and escape from casirivimab. Color dots are all amino acid substitution at the indicated major casirivimab antigen sites. (**D**) Heatmaps illustrating how all single mutations that Omicron obtains affect its escape from vaccinated sera (left). Open squares are Omicron-carrying mutation. Correlation in mutation effects on infectivity and escape from vaccinated sera. (**E**) Dot plots showing the correlation between infectivity and escape value from engineered ACE2. Heatmap squares are colored by mutational effect according to scale bars on the right, with blue indicating deleterious mutations. Heatmaps of the whole spike are available in supplementary figure 4.

Supplementary Materials

The PDF file includes:

Figs. S1 to S5

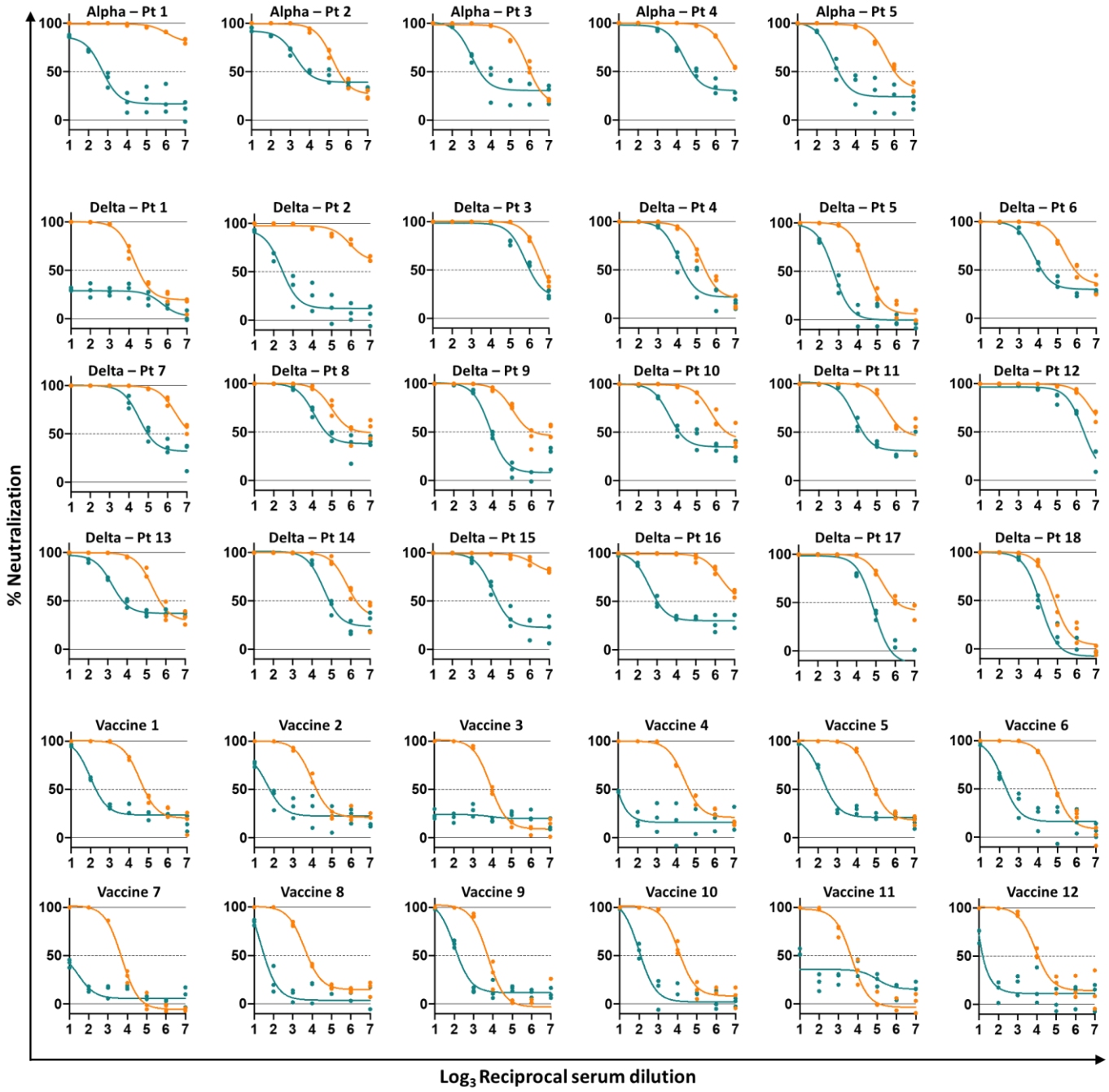

Fig.S1. Neutralization assay with Omicron pseudovirus.

Individual data for Figure 1A to 1C. Neutralization of the parental pseudovirus (red) and Omicron (green) analyzed in 293T/ACE2 cells. n = 3 technical replicates.

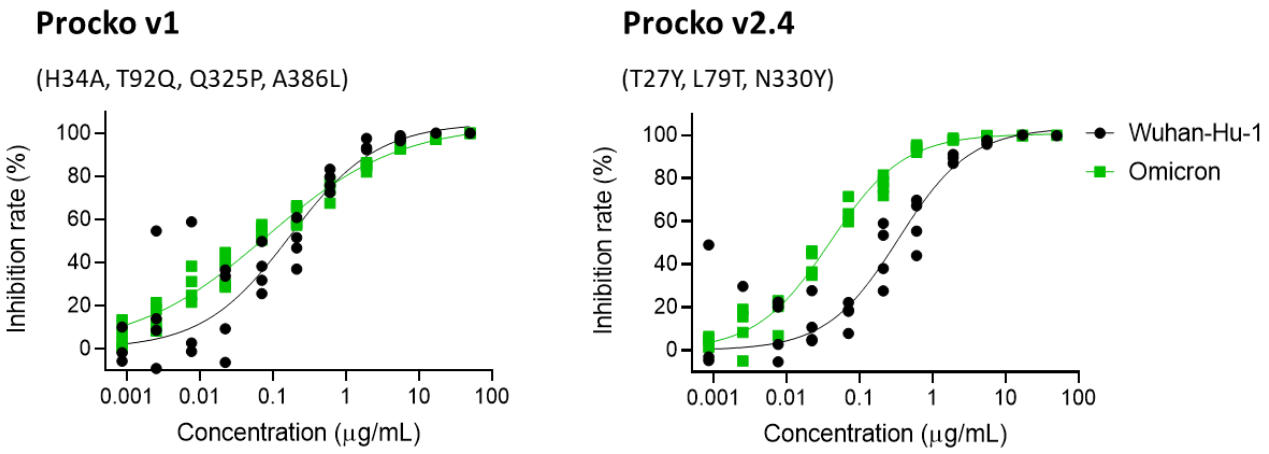

Fig.S2. Neutralization assay for engineered ACE2 reported by Procko.

Neutralization efficacy of v1 and v2.4 in the paper reported by Procko; two different ACE2 mutants against Omicron pseudovirus analyzed in 293T/ACE2 cells. n = 4 technical replicates.

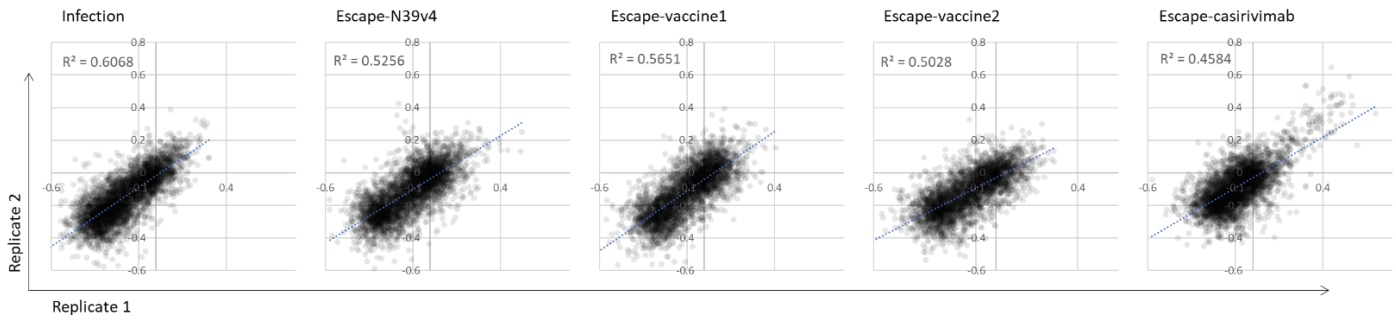

Fig.S3. Reproducibility of each deep Mutational Scan for infectivity and escapes from neutralizing agents, Related to Figure 6.

Correlation in mutation effects on the alteration of infectivity or escape from each neutralizing agent across replicates.

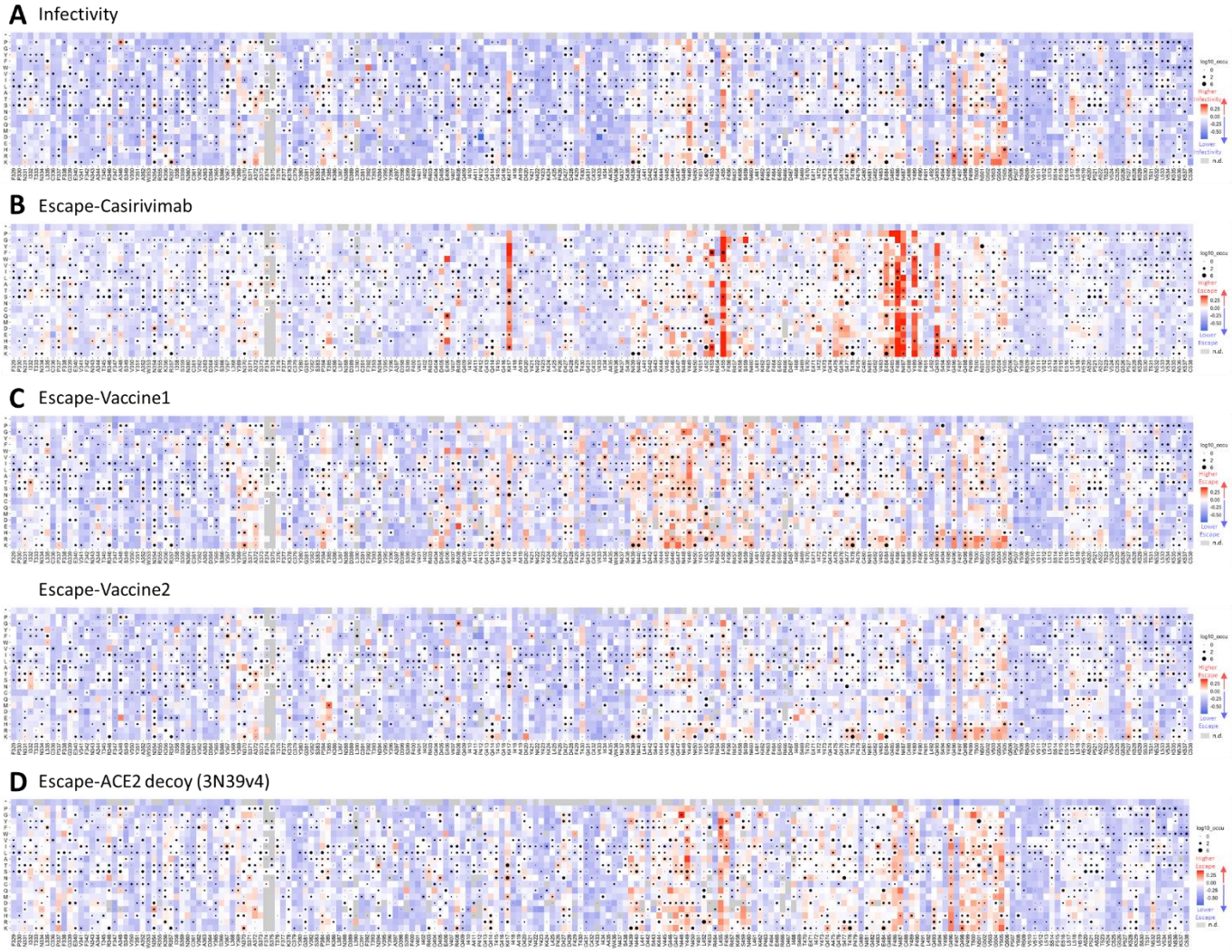

Fig.S4. Sequence-to-Phenotype Maps of the whole RBD, Related to Figure 6.

(**A**-**D**) Heatmaps illuminating how all single mutations affects infectivity (A), escape from casirivimab (B), vaccinated sera (C) and engineered ACE2 (D). Squares are colored by mutational effect according to scale bars on the right, with blue indicating deleterious mutations. Black dot size reflects the frequency in the virus genome sequence according to GISAID database. All dataset is available at Spike DB (https://sysimm.ifrec.osaka-u.ac.jp/sarscov2_dms/).

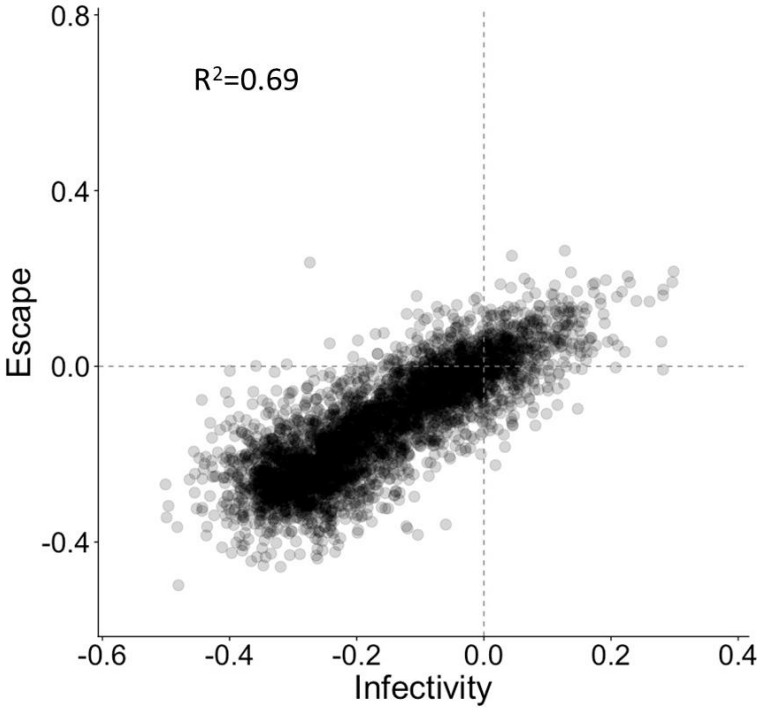

Fig.S5. Reproducibility of correlation between infectivity and escape in the vaccinated sera, Related to Figure 6. Correlation in mutation effects on the alteration of infectivity or escape from the neutralization by sera from different vaccinated individual.